Available online at www.sciencedirect.com
SCIENCE DIRECT
Colloids and Surfaces B: Biointerfaces 50 (2006) 152–159
COLLOIDS AND SURFACES B
www.elsevier.com/locate/colsurfb

Microbial adhesion to zirconium alloys

J.D. Ehrman [a], E.T. Bender [a], N. Stojilovic [a], T. Sullivan [a], R.D. Ramsier [a,*], B.W. Buczynski [b], M.M. Kory [b], R.P. Steiner [c]

[a] *Departments of Physics and Chemistry, The University of Akron, Akron, OH 44325, United States*
[b] *Department of Biology, The University of Akron, Akron, OH 44325, United States*
[c] *Department of Statistics, The University of Akron, Akron, OH 44325, United States*

Received 4 January 2006; received in revised form 31 March 2006; accepted 19 April 2006
Available online 5 May 2006

Abstract

We present data and analyses concerning the adhesion of clinically relevant *Staphylococcus aureus, Staphylococcus epidermidis*, and *Pseudomonas aeruginosa* (bacteria) and *Candida albicans* (yeast) to Zircaloy-2 (Zry-2) and Zircadyne-705 (Zr705) surfaces. These zirconium-based materials are similar to those now being used in total hip and knee replacements. Here we study clinical strains of microbes under shaken and stationary exposure conditions, and their ability to adhere to Zr surfaces having different oxide thicknesses. We use X-ray photoelectron spectroscopy (XPS), scanning electron microscopy (SEM), viable counts, endotoxin assays, and statistical analysis methods, and demonstrate a predictive model for microbial adhesion based on XPS data.

Keywords: Microbial adhesion; Zirconium alloys; Endotoxin; Yeast; Gram negative; Gram positive; Oxidation; XPS

1. Introduction

Zirconium-based materials, similar to those now being used in total hip replacements (THR) and total knee replacements (TKR) [1–4], are the focus of this study. The oxide layer that forms on the surface of zirconium and its alloys is known to be chemically stable in many environments, with good mechanical strength and excellent wear and corrosion resistance. The question is whether the chemical properties of this oxide layer make these materials compatible for use in biomedical applications. Zirconia (ZrO_2, zirconium oxide) ceramic ball heads are commonly found in THR device designs because of good wear and biocompatibility properties [5], and it might be presumed that oxidized Zr would behave similarly. However, these ceramic materials are stabilized into the tetragonal phase by the addition of other oxides such as yttria, but the oxides grown on zirconium alloys are predominantly in the monoclinic phase and are substoichiometric (ZrO_x, $x < 2$).

Although it appears that oxidized Zr alloys exhibit superior wear behavior [1–4], there is little direct evidence that their oxide layers are biocompatible. For example, Olmedo et al. [6] studied the dissemination of zirconium in rats and detected intracellular aggregates of zirconium particles in peritoneum, liver, lung and spleen. They reported that zirconium dissemination is active throughout the body and particles target vital organs. Thus, it is vitally important that we investigate the biocompatibility of Zr-based materials that are being introduced into the human body in the form of prosthetics. Our findings to date [7,8] indicate that understanding and controlling the adhesion of microbial species on these surfaces is not straightforward, and that synergistic effects dominate.

The present study builds on and expands our growing body of knowledge and experience with microbial adhesion on zirconium alloy surfaces. We present data and analyses concerning the propensity of clinically relevant *Staphylococcus aureus, Staphylococcus epidermidis*, and *Pseudomonas aeruginosa* (bacteria) and *Candida albicans* (yeast) to adhere to Zircaloy-2 (Zry-2) and Zircadyne-705 (Zr705) surfaces. Here we study clinical strains of microbes under shaken and stationary exposure conditions, and different surface oxide thicknesses. The choice of microbes includes those found in hospitals and both Gram-positive and

* Corresponding author. Tel.: +1 330 972 4936; fax: +1 330 972 6918.
E-mail address: rex@uakron.edu (R.D. Ramsier).

0927-7765/$ – see front matter © 2006 Elsevier B.V. All rights reserved.
doi:10.1016/j.colsurfb.2006.04.010

-negative genera. We use X-ray photoelectron spectroscopy (XPS), scanning electron microscopy (SEM), viable counts, endotoxin assays, and statistical analysis methods, and discuss trends that are both experimentally and statistically significant.

2. Experimental details

The alloys Zr705 (nominally 2.5% Nb, balance Zr + Hf) and Zry-2 (nominally 1.4% Sn, Hf depleted, balance Zr) were received from Wah Chang (Albany, OR) in the form of sheet stock (approximately 1.0 mm thick) and cut into nominally rectangular coupons. For viable counts and endotoxin assay experiments the coupons were approximately 20 mm × 48 mm, whereas those for XPS and SEM were smaller (approximately 5 mm × 20 mm). Each substrate was polished on one side using diamond pastes followed by a 0.05 μm alumina suspension. The samples were then ultrasonically cleaned, degreased with acetone, and placed in Petri dishes until needed. These samples, that were not deliberately oxidized, are referred to as metallic.

For the deliberately oxidized samples, a convection furnace was used. Polished and cleaned samples from the Petri dishes were placed in the pre-heated furnace. Then, after pre-specified lengths of time, the samples were removed from the hot furnace and allowed to cool in air at a relative humidity of approximately 50%. Annealing temperatures were in the range 500–600 °C, and more details about this oxidation procedure are available elsewhere [7–10]. Standard X-ray diffraction (XRD) measurements were performed on oxidized substrates, to verify that our oxidation procedure predominantly yields the expected monoclinic form of zirconium oxide on the surfaces [8]. All of the oxide layers that we use are in the thickness range before the transition region in the growth kinetics, where the oxides turn from black to beige and white [10].

Clinical strains of *S. aureus, S. epidermidis, P. aeruginosa* and *C. albicans* were incubated overnight at 37 °C in tryptic soy broth (TSB). The four microbes were tested separately and as a mixture in eight-flask sets. The eight flasks each contained 250 ml of TSB, 0.5 ml of microbes (or 0.13 ml of each in the mixture), and two sample coupons. A stationary four-flask set and a separate shaken (175 rpm) four-flask set were incubated at 37 °C for 3 days and then the broths were carefully removed.

A metal coupon was aseptically removed from each flask and rinsed for one min in separate 250 ml beakers of sterile saline (0.85 wt.%/vol.) solution. Each rinsed coupon was then put into a tube of sterile saline and vortexed for one min, allowed to sit for approximately five min, and then vortexed for an additional min. The second coupon in each flask was aseptically rinsed in a corresponding beaker of sterile water and placed on sterile bibulous paper in a sterile glass Petri dish for surface analysis. The latter procedure avoided the use of saline solution as a rinsing agent, since this would contaminate the surfaces studied by XPS and microscopy. The microbes in the saline tubes were diluted and plated using the spread plate technique. Total dilutions of 2×10^1 to 2×10^7 in sterile saline were used and plated on tryptic soy agar (TSA). The plates were incubated at 37 °C overnight. Viable counts were reported as the number of microbes per ml.

The XPS analysis was performed in fixed analyzer transmission mode under high vacuum conditions (pressures often below 8×10^{-9} Torr) using a Kratos ES-300 electron spectrometer with a dual anode X-ray source. For all measurements, the aluminum source was used for the primary survey and detail scans, however the magnesium anode was sometimes used to verify the identity of some Auger features. The X-ray source was operated at 12 kV with emission currents in the range 7–10 mA, and the samples were approximately 1 cm away from the source. Samples were mounted onto the end of a probe inserted through a load-lock sample transfer flange. Focused and rastered argon ion sputtering (2.5 keV) was performed to remove surface contamination and to depth profile. Ultra-high purity argon at a pressure of 2×10^{-5} Torr was used, which corresponds to a sputtering rate of a gold standard of approximately 0.63 nm/min. Microscopic imaging of some of the surfaces was performed with optical and SEM techniques.

The Limulus Amebocyte Lysate (LAL) gel clot assay (BioWhittaker, Walkersville, MD) was used to detect Gram negative bacterial endotoxin. The endotoxin is a portion of the lipopolysaccharide of the outer membrane of the Gram negative cell wall. In most Gram negative bacteria, the endotoxin is exposed upon cell lysis. The lysate contains amebocytes (leukocytes) from the horseshoe crab (*Limulus polyphenus*). Bacterial endotoxin catalyzes a reaction that produces coagulase, an enzyme which hydrolyzes coagulogen (a protein in the amebocyte lysate) resulting in a detectable clot [11]. The LAL gel clot assay is validated by the FDA as an end product endotoxin test [12].

For LAL studies, clinical microbes were incubated with the metal coupons under stationary or shaken conditions and the metal coupons were washed in saline as previously described. The microbes were removed from the saline by five min centrifugation in a microfuge, and the supernatants were stored at 5 °C. All extraneous endotoxin on the glassware was presumably destroyed by autoclaving and baking the glassware at 180 °C for four hr. The water, lysate and plastic-ware used in the assays were endotoxin-free. The test amebocyte lysate was prepared by adding 1.8 ml of endotoxin-free water to the 16-test vial of lyophilized lysate. The endotoxin positive control was 10 ng of *E. coli* endotoxin standard hydrated with 5.0 ml of endotoxin-free water. This standard had a potency of 20 EU/ml and was diluted with endotoxin-free water to 1 EU/ml for use as a positive control. The negative control was endotoxin-free water.

An endotoxin test assay tube contained 0.1 ml of test sample (positive control, negative control or experimental) and 0.1 ml of lysate, and was incubated for one hr in a 37 °C heating block. The positive controls were the 1 EU/ml endotoxin diluted with endotoxin-free water by a series of five 1:2 dilutions to 1:32 and lysate was added to each dilution tube. The experimental samples were diluted to 1:32 by five series of 1:2 dilutions using endotoxin-free water. Lysate was added to each diluted sample. A positive reaction was a clot with the endpoint being the positive tube containing the most dilute sample.

3. Results and discussion

3.1. XPS

Although XPS must be done in vacuum, it is a very powerful tool for the study of biological systems and their interaction with other materials [13–16]. It offers surface chemical information, and can be used to quantify the presence of biological species on surfaces. Adventitious carbon is always present, but adsorbed species containing nitrogen moieties can be detected. Sputter depth profiling can also be performed through biofilms to assess their propensity to form heterogeneous layers. XPS survey scans are shown in Fig. 1. The top panel (A) is from metallic Zr705, and the bottom panel (B) is from Zr705 with a two micron thick oxide layer. Both samples were exposed to *S. epidermidis* in TSB for three days under shaken conditions. The main features present are from zirconium, oxygen, nitrogen and carbon, as expected. Traces of sodium are also evident.

Bacterial adhesion results in a decrease in the Zr features due to electron scattering by adsorbates and is a consistent trend that we have observed, which is similar to the study by Rubio et al. [17]. This is quantified by the insets in the panels of Fig. 1. The photoelectron spectral features were integrated and corrected for element-specific sensitivity factors. The resulting signal ratios (O:Zr, N:Zr, and C:Zr) for Fig. 1(A) are about five times larger than those determined from Fig. 1(B). A simple interpretation of these data is that more bacteria are adsorbed on the metallic surface than on the oxidized sample, consistent with what we have reported previously based on viable counts data [7]. However, such observations based on XPS data do not discriminate between different microbes, so a more robust analysis was performed.

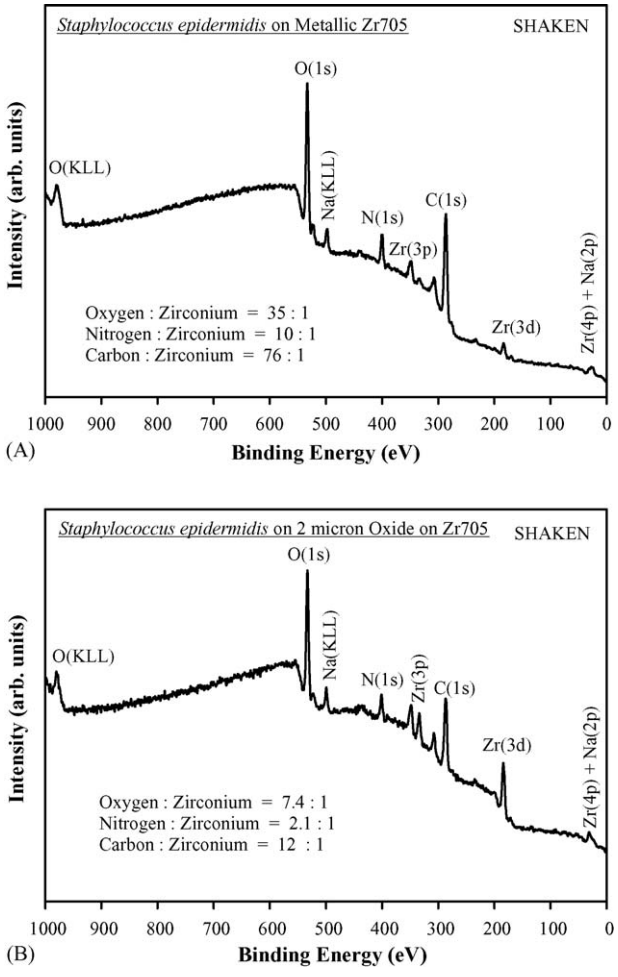

Fig. 1. XPS survey scans following three-day exposures to *Staphylococcus epidermidis* under shaken conditions. Panel A is from a metallic Zr705 substrate, and panel B is from Zr705 with a two-micron thick oxide layer.

The XPS signal ratio data were further analyzed using logistic regression to assess whether the presence of particular organisms could be identified by their elemental signatures derived from XPS. First, a model was constructed in which the outcome variable was organism (*C. albicans, P. aeruginosa, S. epidermidis,* and a mixture of the organisms). The predictors were the integrated areas for carbon, nitrogen, zirconium, and sodium from the XPS data. For each sample, the model produced, for each organism, probabilities that the sample contained that organism (or the mixture). For example, one sample produced the probabilites: $P(C.\ albicans) = 0.045$; $P(P.\ aeruginosa) = 0.952$; $P(S.\ epidermidis) = 0.003$; $P(\text{mixture}) = 1.26 \times 10^{-12}$. The model predicts, or classifies, the sample as containing the organism (or mixture) with the highest probability. The sample in this example, therefore, would be classified as *P. aeruginosa*, and in fact this sample did contain *P. aeruginosa*. Thus, the model correctly classified this sample. Of the 34 samples classified by this model, 27 (79.4%) were correctly classified. Table 1 shows the classification results.

The correctly classified samples lie on the main diagonal of Table 1, while misclassified samples lie off the diagonal. Most of the misclassifications involved the mixture, and it is not surprising that the model would have the most difficulty classifying these samples. To investigate this issue, a second logistic regression model was constructed without the mixture. In this model, the outcome variable was organism (*C. albicans, P. aeruginosa,* and *S. epidermidis*). The predictors were the integrated areas for carbon, nitrogen, and zirconium from the XPS data. Of the 26 samples classified by this model, 24 (92.3%) were correctly classified. Thus we are confident that models of this

Table 1
Classification results for model concerning C, N, Zr, and Na XPS data

Predicted organism				
No. of samples % of total	*S. epidermidis*	*P. aeruginosa*	*C. albicans*	Mixture
Actual organism				
S. epidermidis	8 23.53	0 0.00	0 0.00	0 0.00
P. aeruginosa	0 0.00	8 23.53	1 2.94	1 2.94
C. albicans	0 0.00	0 0.00	6 17.65	2 5.88
Mixture	0 0.00	2 5.88	1 2.94	5 14.71

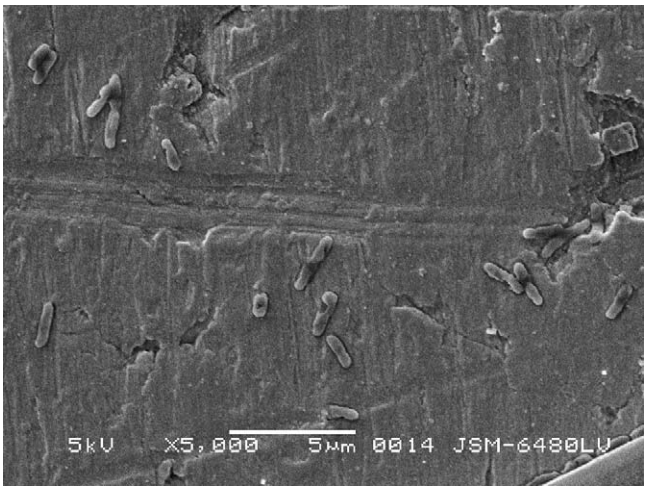

Fig. 2. SEM image of an oxidized Zr705 surface exposed to *Pseudomonas aeruginosa* for three days while shaking.

type based on XPS data can provide useful information once fully-developed.

3.2. SEM

Bacterial adhesion has also been investigated by SEM imaging, as shown in Fig. 2. This is from an oxidized Zr705 surface exposed to *P. aeruginosa* for three days while shaking. As expected, the bacteria have a rod-like appearance [18]. Most of our images show sparsely populated regions of bacteria separated by large regions of essentially no bacteria. This is consistent with the work of Scarano et al. [19], who showed that zirconium oxide disks attracted fewer bacteria than commercially available titanium in a human *in vivo* study, with only about 12% of the surface attracting bacteria.

The image of Fig. 2 and others like it indicate that these bacteria do not preferentially adsorb in regions of surface defects. From the standpoint of the effects of surface preparation on bacteriological adhesion, this must be investigated in greater detail. For example, one study demonstrated that highly-polished zirconia ceramics do not offer an advantage over as-fired materials in terms of bacterial colony growth [20]. On the other hand, the role of surface morphology at the micro- and nano-scales on the attachment of cells is frequently being discussed in the literature [21–29]. Surfaces for prosthetics need to be smooth at articulating regions, and effort has been put into this [30], but the attachment of bone tissue may depend on roughness and defects on the order of one micron in size [31]. The question remains as to whether surface morphology can influence the attachment of microbes to zirconium alloys.

3.3. Endotoxin assays

We are also interested in endotoxin adsorption [32–35] on zirconium alloy surfaces, and the use of endotoxin assays for detecting bacterial adhesion. Fig. 3 shows a plot of results from our assay studies, with the full data set presented in Table 2. As expected, there was no or only 1:2 endotoxin detected in samples

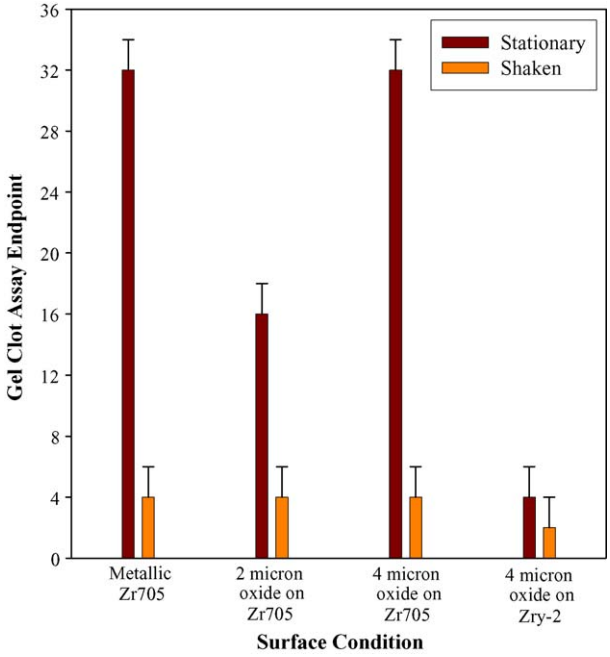

Fig. 3. Results of endotoxin assays from samples exposed to *Pseudomonas aeruginosa* for three days.

of *S. aureus*, *S. epidermidis* or *C. albicans*, as these are Gram positive bacteria and a Gram positive yeast, respectively. Gram positive bacteria and yeasts do not contain endotoxin. Fig. 3 shows that for unoxidized and oxidized Zr705, the amount of detected endotoxin was lower for the shaken samples. These results correlate well with our earlier study [7] where biofilms were formed more readily under stationary (versus shaken) conditions. The uncertainties are from the averaging of two independent runs of each condition.

Note that the detection of *P. aeruginosa* adhesion by these assays requires lysis of the bacterium. This implies there were more dead and lysed *P. aeruginosa* cells in the stationary situation. Whether the stationary conditions actually promoted adhesion, or the shaken conditions removed dead bacteria more readily, is not known at present. Interpretation of the XPS ratios under these two conditions may also depend on such details. Combining the results of various measurement techniques into a self-consistent model of Zr-alloy/biological-species systems will allow us to elucidate the importance of such possible mechanisms.

3.4. Viable counts

Using several different analysis methods permits us to investigate the complementary nature of the data and what they represent. Tables 3 and 4 provide all of the viable counts data collected in this study. These data were analyzed using a three-factor ANOVA. The factors were Organism (*C. albicans*, *S. aureus*, *S. epidermidis*, *P. aeruginosa*, and Mixture), Condition (shaking, stationary), and Material (Zry-2: 4 μm, Zr705: 4 μm, Zr705: 2 μm and unoxidized Zr705). The response variable was microbial growth measured as ln(microbe/ml). The natural logarithm transformation of growth was used to satisfy the ANOVA

Table 2
LAL gel clot assay endpoints with each cell containing data from two independent runs

Metallic Zr705		2 μm Zr705		4 μm Zr705		4 μm Zry-2	
Stationary	Shaken	Stationary	Shaken	Stationary	Shaken	Stationary	Shaken
S. aureus							
1:2	1:2	1:2	1:2	1:2	1:2	1:2	1:2
1:2	0	1:2	1:2	0	0	1:2	0
S. epidermidis							
1:2	1:2	1:2	0	0	0	0	0
0	0	1:2	0	0	0	0	0
P. aeruginosa							
1:32	1:4	1:16	1:4	1:32	1:4	1:4	1:2
1:16	1:4	1:16	1:4	1:32	1:2	1:4	1:2
C. albicans							
0	0	0	0	0	1:2	1:2	1:2
0	0	0	0	0	0	1:2	0
Mixture							
1:16	1:2	1:16	1:4	1:8	0	1:8	0
1:16	1:4	1:16	1:4	1:8	0	1:8	0

requirements of normally distributed data with equal variability across factor levels.

First, a model including main effects for each factor, all two-factor interactions, and the three-factor interaction was tested. In this model (mean square error = 0.404, error d.f. = 40), all interactions and main effects were significant ($P < 0.008$). The three-way interaction is graphed in Fig. 4. We observed overall greater growth under stationary conditions versus shaken conditions, especially of *S. epidermidis* and *C. albicans*.

P. aeruginosa and *S. aureus* exhibited less difference in growth between shaken and stationary conditions, except on Zr705: 2 μm samples, where there was considerably greater growth under stationary conditions. Growth of the yeast, *C. albicans,* showed little difference among the material surfaces. The mixture of organisms displayed greater growth overall than the single-organism cultures. In addition, the mixture exhibited little difference in growth between the shaken and stationary conditions, except for Zr705: 4 μm surfaces, on which growth was considerably less under shaken conditions.

Fig. 5 demonstrates that overall, averaging over the different microbes and the mixture, stationary exposures resulted in much higher growth ($P < 0.05$; Tukey's HSD test) than shaken conditions for all surfaces. This analysis therefore supports the findings of the previous section based on endotoxin assays alone, and also our previous work [7]. In addition, we see from Fig. 5 that under stationary conditions, microbial attachment is most pronounced on Zr705 with a 2 μm thick oxide layer (this is especially true of *P. aeruginosa* and *S. aureus*; see Fig. 4), and is least effective on Zr705 with a 4 μm thick oxide under shaken conditions (most notably for the mixture; see Fig. 4).

Further results from the ANOVA analyses are presented in Fig. 6. It is apparent that all microbes and the mixture

Table 3
Viable counts (# microbes/ml) from stationary conditions

Run	Metallic Zr705	2 μm Zr705	4 μm Zr705	4 μm Zry-2
S. aureus				
1	1.60×10^3	2.02×10^5	4.60×10^3	6.20×10^2
2	1.16×10^3	9.16×10^4	7.60×10^3	6.04×10^2
S. epidermidis				
1	6.48×10^4	7.50×10^4	9.80×10^3	1.52×10^5
2	6.65×10^5	1.22×10^5	1.24×10^4	9.45×10^4
P. aeruginosa				
1	2.75×10^4	5.10×10^5	2.97×10^4	4.10×10^4
2	5.91×10^4	5.15×10^5	1.90×10^4	4.85×10^4
C. albicans				
1	6.08×10^3	5.44×10^3	6.28×10^3	6.86×10^3
2	1.54×10^4	1.10×10^4	9.80×10^3	6.80×10^3
Mixture				
1	3.93×10^4	3.06×10^5	1.64×10^5	3.64×10^4
2	7.00×10^4	5.60×10^4	2.39×10^5	1.33×10^5

Table 4
Viable counts (# microbes/ml) from shaken conditions

Run	Metallic Zr705	2 μm Zr705	4 μm Zr705	4 μm Zry-2
S. aureus				
1	2.74×10^3	2.00×10^3	6.00×10^3	1.30×10^3
2	2.05×10^3	9.20×10^3	2.75×10^3	4.50×10^2
S. epidermidis				
1	$<6.00 \times 10^2$	$<6.00 \times 10^2$	$<6.00 \times 10^2$	$<6.00 \times 10^2$
2	6.20×10^2	1.75×10^3	$<6.00 \times 10^2$	2.60×10^3
P. aeruginosa				
1	1.24×10^4	9.20×10^3	8.30×10^3	8.60×10^3
2	1.16×10^4	8.20×10^3	7.75×10^3	9.45×10^3
C. albicans				
1	$<6.00 \times 10^2$	$<6.00 \times 10^2$	6.20×10^2	6.00×10^2
2	3.78×10^3	2.00×10^3	8.40×10^2	1.96×10^3
Mixture				
1	9.55×10^4	1.75×10^5	1.40×10^3	5.94×10^4
2	1.45×10^5	9.60×10^4	9.25×10^3	7.66×10^4

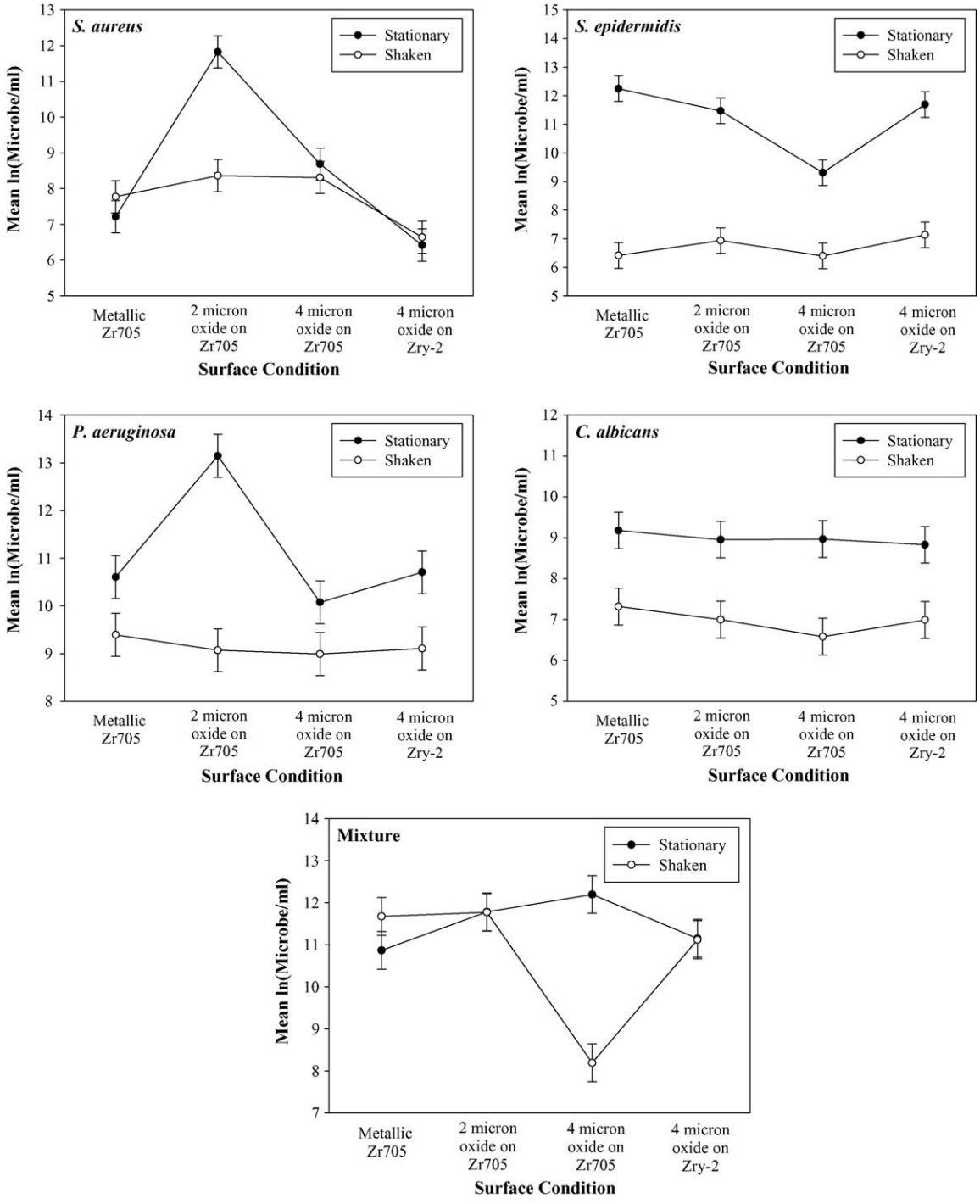

Fig. 4. ANOVA interaction plots for each organism, comparing mean growth under shaken and stationary conditions for different surfaces.

of species adhere more readily during stationary rather than shaken exposures, averaging over the different adherent surfaces. Growth from the mixture is much greater than for all individual species under shaken conditions ($P < 0.05$; Tukey's HSD test), but under stationary conditions the differences tend to be smaller. It is interesting that the growth trends under stationary conditions (mixture ~ *P. aeruginosa* ~ *S. epidermidis* ≫ *C. albicans* ~ *S. aureus*) differ from those under shaken conditions (mixture > *P. aeruginosa* > *S. aureus* > *C. albicans* ~ *S. epidermidis*). This indicates that synergistic effects concerning the adsorption/desorption of microbes from these surfaces are present.

In addition to total hip and knee replacement applications of zirconium alloys, there are recent literature reports which indicate that Zr-based coatings are also being investigated for biomedical uses [36–38]. This makes our studies even more relevant and timely, and necessarily requires that we investigate the adhesion and growth of fungi and endotoxins as well as

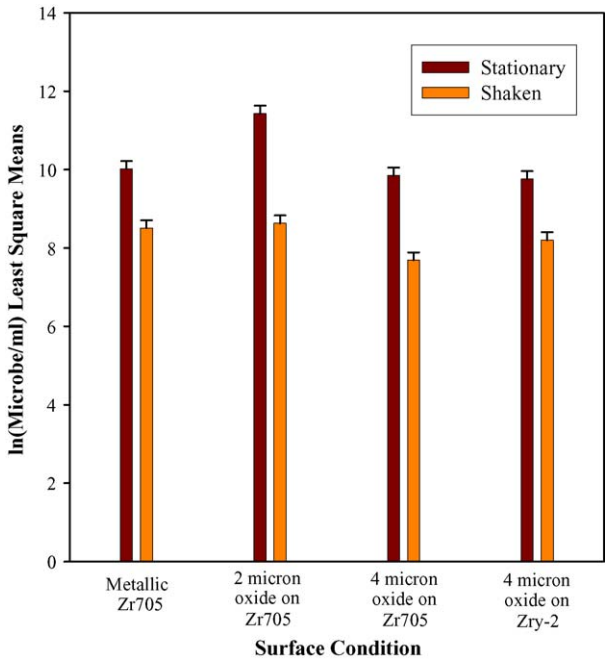

Fig. 5. ANOVA results indicating that microbial adhesion under stationary conditions dominates (over shaken) for all surfaces studied here.

clinically relevant bacteria. It is also important to realize that all of the relevant Zr alloys are predominantly in the alpha phase, e.g., the metal crystal structure is hexagonal close packed. What this means is that there is an anisotropy that will be exhibited in extruded or rolled materials. The rolling or extruding direction will align the long axis of the metal grains, which will still play a role once the material is oxidized to provide the protective coating.

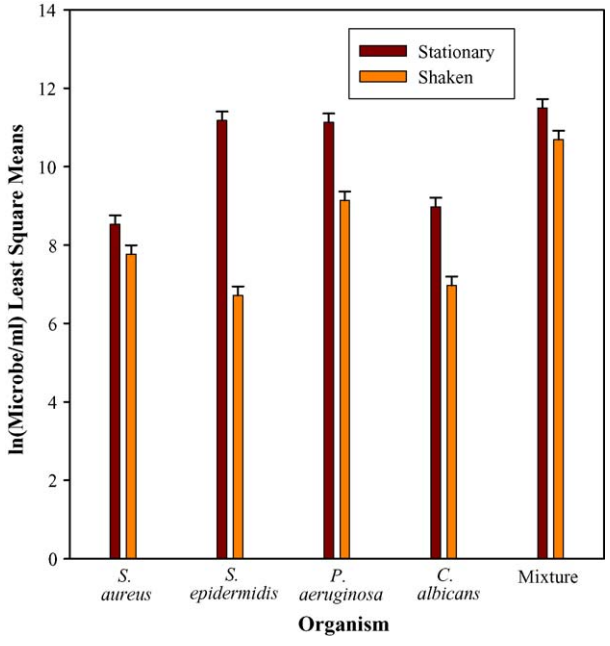

Fig. 6. ANOVA results indicating that the mixture of species adheres most effectively vs. the individual species, with statistically significant differences under shaken exposure conditions.

4. Summary

In this study we presented a model that has the ability to predict the identity of microbial species adsorbed on Zr alloy surfaces based on XPS signal ratio data. We have also shown that we can discriminate between the adsorption of Gram negative and Gram positive species on Zr alloy surfaces using endotoxin assays. Finally, ANOVA and viable counts methods were used to demonstrate that stationary exposures result in significantly larger quantities of microbes adhered to Zr alloy surfaces than do shaken exposure conditions.

Acknowledgements

We acknowledge support for this effort through NIH-NIBIB grant number EB003397-01, and we are grateful to Wah Chang for providing the Zry-2 and Zr705 materials free-of-charge. We are also appreciative of the assistance provided by Jeannette Killius of the Northeastern Ohio Universities College of Medicine with the SEM phases of this work. Finally, we thank our collaborators Mark Kovacik and Richard Mostardi of the Walter A. Hoyt Jr. Musculoskeletal Research Laboratory, Department of Orthopedics, Summa Health System, for their help throughout the course of this work.

References

[1] M.D. Ries, A. Salehi, K. Widding, G. Hunter, J. Bone Joint Surg. 84A (Supp. 2) (2002) 129.
[2] M. Spector, M.D. Ries, R.B. Bourne, W.S. Sauer, M. Long, G. Hunter, J. Bone Joint Surg. 83-A (2001) 80.
[3] V. Benezra, S. Mangin, M. Treska, M. Spector, G. Hunter, L.W. Hobbs, Mater. Res. Soc. Symp. Proc. 550 (1999) 337.
[4] A.M. Patel, M. Spector, Biomaterials 18 (1997) 441.
[5] C. Piconi, G. Maccauro, Biomaterials 20 (1999) 1.
[6] D. Olmedo, M.B. Guglielmotti, R.L. Cabrini, J. Mater. Sci.: Mater. Med. 13 (2002) 793.
[7] B.W. Buczynski, M.M. Kory, R.P. Steiner, T.A. Kittinger, R.D. Ramsier, Coll. Surf. B: Biointerf. 30 (2003) 167.
[8] E.A. Yamokoski, B.W. Buczynski, N. Stojilovic, J.W. Seabolt, L.M. Bloe, R. Foster, N. Zito, M.M. Kory, R.P. Steiner, R.D. Ramsier, J. ASTM Intern. 2(7), July/August (2005), paper ID JAI12812. [Reprinted in Titanium, Niobium, Zirconium, and Tantalum for Medical and Surgical Applications, L.D. Zardiackas, M.J. Kraay and H.L. Freese (Eds.), pp. 225–238 (ASTM Int., West Conshohocken, PA, 2006)].
[9] J.M. Morgan, J.S. McNatt, M.J. Shepard, N. Farkas, R.D. Ramsier, J. Appl. Phys. 91 (2002) 9375.
[10] J.S. McNatt, M.J. Shepard, N. Farkas, J.M. Morgan, R.D. Ramsier, J. Phys. D: Appl. Phys. 35 (2002) 1855.
[11] N.S. Young, J. Levin, R.A. Prendergast, J. Clin. Invest. 51 (1972) 1790.
[12] Guideline on Validation of the Limulus Amebocyte Lysate Test as an Endproduct Endotoxin Test for Human and Animal Parenteral Drugs, Biological Products, and Medical Devices, U.S. Department of Health and Human Services, Public Health Service, Food and Drug Administration, 1987.
[13] H. McCormick, R. McMillan, K. Merrett, F. Bensebaa, Y. Deslandes, M.A. Dube, H. Sheardown, Coll. Surf. B: Biointerf. 26 (2002) 351.
[14] M.P. Casaletto, S. Kaciulis, G. Mattogno, A. Mezzi, L. Ambrosio, F. Branda, Surf. Interf. Anal. 34 (2002) 45.
[15] J.C. Tokash, N. Stojilovic, R.D. Ramsier, M.W. Kovacik, R.A. Mostardi, Surf. Interf. Anal. 37 (2005) 379.
[16] N. Stojilovic, J.D. Ehrman, E.T. Bender, J.C. Tokash, R.D. Ramsier, M.W. Kovacik, Appl. Surf. Sci. 252 (2006) 3760.

[17] C. Rubio, D. Costa, M.N. Bellon-Fontaine, P. Relkin, C.M. Pradier, P. Marcus, Coll. Surf. B: Biointerf. 24 (2002) 193.
[18] G. Reid, H.J. Busscher, S. Sharma, M.W. Mittelman, S. McIntyre, Surf. Sci. Rep. 21 (1995) 251.
[19] A. Scarano, M. Piattelli, S. Caputi, G.A. Favero, A. Piattelli, J. Periodontol. 75 (2004) 292.
[20] L. Rimondini, L. Cerroni, A. Carrassi, P. Torricelli, Int. J. Oral Maxillofac. Implants 17 (2002) 793.
[21] R.G. Fleming, C.J. Murphy, G.A. Abrams, S.L. Goodman, P.F. Nealey, Biomaterials 20 (1999) 573.
[22] R. Barbucci, S. Lamponi, A. Magnani, D. Pasqui, Biomol. Eng. 19 (2002) 161.
[23] R. Barbucci, D. Pasqui, A. Wirsen, S. Affrossman, A. Curtis, C. Tetta, J. Mater. Sci.: Mater. Med. 14 (2003) 721.
[24] B. Zhu, Q. Zhang, Q. Lu, Y. Xu, J. Yin, J. Hu, Z. Wang, Biomaterials 25 (2004) 4215.
[25] A.I. Teixeira, G.A. Abrams, P.J. Bertics, C.J. Murphy, P.F. Nealey, J. Cell Sci. 116 (2003) 1881.
[26] C.C. Berry, G. Campbell, A. Spadiccino, M. Robertson, A.S.G. Curtis, Biomaterials 25 (2004) 5781.
[27] A.-S. Andersson, F. Backhed, A. von Euler, A. Richter-Dahlfors, D. Sutherland, B. Kasemo, Biomaterials 24 (2004) 3427.
[28] O. Zinger, K. Anselme, A. Denzer, P. Habersetzer, M. Wieland, J. Jeanfils, P. Hardouin, D. Landolt, Biomaterials 25 (2004) 2695.
[29] A.-S. Andersson, P. Olsson, U. Lidberg, D. Sutherland, Exp. Cell Res. 288 (2003) 177.
[30] D. Heuer, A. Harrision, H. Gupta, G. Hunter, Bioceram., 15 Key Eng. Mater. 240–242 (2003) 789.
[31] P. Thomsen, C. Larsson, L.E. Ericson, L. Sennerby, J. Lausmaa, B. Kasemo, J. Mater. Sci.: Mater. Med. 8 (1997) 653.
[32] J.M. Seabold, J.L. Nalepka, V.M. Goldberg, M.C. Stewart, E.M. Greenfield, in: Proceedings of the 49th Annual Meeting of the Orthopaedic Research Society, Paper #0285, 2003.
[33] J.L. Nalepka, V.M. Goldberg, J.E. Dennis, E.M. Greenfield, in: Proceedings of the 49th Annual Meeting of the Orthopaedic Research Society, Paper #1373, 2003.
[34] Y. Aoto, H. An, Y. Imai, E. Thonar, R. Pichika, M. Lenz, K. Masuda, in: Proceedings of the 49th Annual Meeting of the Orthopaedic Research Society, Paper #1141, 2003.
[35] A.A. Ragab, R. Van de Motter, S.A. Lavish, V.M. Goldberg, J.T. Ninomiya, C.R. Carlin, E.M. Greenfield, J. Orthoped. Res. 17 (1999) 803.
[36] B. Groessner-Schreiber, M. Hannig, A. Duck, M. Griepentrog, D.F. Wenderot, Eur. J. Oral Sci. 112 (2004) 516.
[37] R. Lappalainen, S.S. Santavirta, Clin. Orthoped. Rel. Res. 430 (2005) 72.
[38] L.I. Mikhalovska, M. Santin, S.P. Denyer, A.W. Lloyd, D.G. Teer, S. Field, S. Mikhalovsky, Thromb. Haemost. 92 (2004) 1032.